Hindawi
Geofluids
Volume 2019, Article ID 5368765, 13 pages
https://doi.org/10.1155/2019/5368765

Research Article

Physical Tank Experiment Investigation on Rainfall Producing Groundwater Level in Homogeneous Material Slopes

Chao Zhang[1], **Wei Shao**[2,3], **Fucai Yue**[2], **Pooya Saffari**[2] and **Wen Nie**[2]

[1]*State Key Laboratory of Geomechanics and Geotechnical Engineering, Institute of Rock and Soil Mechanics, Chinese Academy of Sciences, Wuhan 430071, China*
[2]*Quanzhou Institute of Equipment Manufacturing, Haixi Institutes, Chinese Academy of Sciences, Quanzhou, Fujian 362000, China*
[3]*School of Hydrology and Water Resources, Nanjing University of Information Science and Technology, Nanjing, 210044 Jiangsu, China*

Correspondence should be addressed to Wen Nie; wen.nie@fjirsm.ac.cn

Received 11 November 2018; Revised 22 February 2019; Accepted 2 April 2019; Published 7 May 2019

Guest Editor: Massimiliano Bordoni

It has been recognized that pore water pressure (PWP) changes in response to precipitation play a critical role in rainfall-triggered landslides. Tank models as a kind of undetermined model are widely applied for estimating groundwater levels in slopes. Most of these applications treat the tank models as a theoretical model. Therefore, in this study, physical tank experiments are reported, indicating an evaluation of three typical conceptual tank models (i.e., simple tank model, surface runoff tank model, and lateral water flow supply tank model). To reduce the slope structure controlling affection, the study takes homogenous soil material as the simulation of the slope mass. The experimental results demonstrated how the groundwater tables producing pore water pressure were affected by infiltration time lags, surface runoff, and lateral flow.

1. Introduction

Landslides are important and widespread natural hazards within alpine regions and can have significant impacts on human lives and infrastructures. Pore water pressure plays an important role in determining the stability of rainfall-triggered landslides. The increase of pore water pressure may reach positive values that are highly undesirable for slope stability, while, for unsaturated soil slopes, the change of pore water pressure caused by rainfall infiltration is an important triggering factor of landslides. A series of small-scale slope experiments highlight that the presence of coarse-textured unsaturated pumiceous layers, interbedded between finer ashy layers, can delay the wetting front advancement, thus initially confining the infiltration process within the finer uppermost layer [1]. Soil water content is the result of multifactor interactions, and proper soil water retention curves and hydraulic conductivity functions are necessary for a correct analysis of groundwater flow in unsaturated slopes [2]; however, measurement of soil water content is time consuming and costly. In addition, there is no mathematical relationship between pore water pressure and the related parameters [3]. Therefore, it is required to establish hydrological models to estimate the pore water pressure in slopes. The hydrological models can be deterministic or based on an optimized method. The deterministic hydrological model commonly uses Darcy-Richards or Boussinesq equations to simulate the groundwater flow in slopes [4]. Or some models can describe the interaction between the soil and atmosphere in pyroclastic soils with a view to understanding whether and to what extent the prediction of the hydraulic (and mechanical) behavior of geotechnical problems regulated by rainfall-induced fluctuations of matric suction is influenced by evaporation phenomena [5]. However, the method is usually computationally intensive, and the application needs a detailed investigation of the geometries and hydraulic properties of the soil material [6]. In contrast with the deterministic model, the model based on the optimized method does not normally require detailed information on hydraulic properties of the slope

material such as permeability and infiltration. In the model, the historical data are used for estimating the parameters of the defined model structure [7, 8]. The pore water pressure and the groundwater level can be determined from these parameters. The method is applicable to a wide range of slopes. A tank model is a nonlinear theorized calculation optimized model used to describe the behaviors of water hydraulic properties [9]. The simple tank model [9], surface runoff tank model [10], and lateral water flow supply tank model [11, 12] are the three typical types of this model. The widely used simple tank model is a complex linear theorized calculation [9]. It is based on the water balance theory that tracks water into and out of a particular area of interest. The model can be used for calculation of pore water pressure in porous media. The 1D simple tank model usually can simulate the groundwater level of one point in a shallow slope without considering the lateral water flow supply [9]. In order to consider the lateral groundwater flow, infiltration time lag, and surface runoff, a multistorage tank model (such as the surface runoff tank model and lateral water flow supply tank model) is needed. The multistorage tank model can estimate the groundwater fluctuations of landslides caused by heavy rainfall [10–12]. The distinct properties of the three tank models are as shown in Table 1.

The simple tank model is easy to implement with high computational efficiency. However, its applications were limited to a low slope angle (one point for the pore water pressure (PWP) represents the entire water table level) and high porosity and permeability soil materials without considering surface runoff. The surface runoff tank models can overcome the limitations from surface infiltration rates and enable a simulation of the surface runoff generated by the excess infiltration rainwater [13]. The lateral water supply tank model can be applied for any slope angle, but its complicated structure produces a higher systematically cumulative error. The highlight of the application of the tank model is using a simple model structure with as-little-as-possible model parameters to describe the water balance including water content and groundwater level [14, 15]. Unfortunately, most applications of the tank model are still a theoretic model and require many parameters for calibration. As a "grey model," there are few direct physical experiments about the investigation of the tank model hydraulic parameters. The tank model based on the optimized method should always seek less, not more, model parameters. Thus, this research aims to investigate the simple hydraulic phenomena under different rainfall events based on physical tank experiments. These investigations would help to construct the tank model with less or limited parameters and a simple structure. In this study, physical tank experiments are employed to investigate the relationships between rainfall events and groundwater pressure ignoring the infiltration process in the homogenous soil materials as the simulation of slope mass during the rainfall events [14] (Figure 1), and only a few parameters (rainfall and groundwater pressure) were used to constrain the tank model for the estimation of pore water pressure.

Table 1: Characters of the three typical tank models.

Type	Characters of applications
Simple tank model [9]	Simple model; assumed low slope angle; no surface runoff; negligible lateral water flow supply
Surface runoff tank model [10]	Considering surface runoff; requires maximum infiltration rate test; less lateral water flow supply
Lateral water flow supply tank model [11, 12]	Increasing model complex; relatively high error; any slope angle

2. Methods

2.1. Test Setup and Testing Materials

2.1.1. Physical Tank Models. A series of physical tank model systems made of plexiglass was conducted, and the hydrological behavior of a slope mass, representing a homogenous hillslope, was investigated (Figure 1). In order to shape the slope mass, the soil was filled inside the tank in layers of 5 cm height. A plate squeezed the soil mass by applying 120 N force to each soil layer (Figure 2).

2.1.2. Rainfall Simulator. For the purpose of rainfall simulations, the rainfall intensity test and uniform degree test of rainfall are necessary before the experiments. A water pump was installed to increase water pressure and supply artificial rainfall through nozzles (uniformity coefficient was ~0.87). The pump can adjust the water pressure between the water input and output by a pressure-increasing valve. The spray nozzles can produce the uniform misty rainfall. A flowmeter between the pump and nozzles steadily controlled the rainfall intensity (10–250 ml/min) by a flow adjustment. A water storage tank was used for the water supply. The level of water inside the tank was measured with a ruler which was placed on the edge of the tank. The rainfall simulator is shown in Figure 3.

2.1.3. Rainfall Intensity Test. A simple tank with dimensions of 300 × 300 × 300 mm was used in order to test the rainfall intensity. The collected simulation rainfall in unit time is compared to the calculated rainfall depending on the flowmeter. The flow rates of the flowmeter were 15 to 120 ml/min and the increment value was 15 ml/min. Each test lasted 0.5 hr. The test results are shown in Figure 4.

2.1.4. Uniform Degree Test of Simulation Rainfall. Generally, the uniformity coefficient of a stable rainfall simulation should be greater than 0.8 [16]. The uniform degree of rainfall can be calculated as follows:

$$k = 1 - \sum_{i=1}^{n} \frac{|x_i - x|}{nx}, \quad (1)$$

where k is the uniformity coefficient, x_i is the rainfall at the measurement positions, x is the average rainfall at the measurement positions, and n is the number of measurement positions.

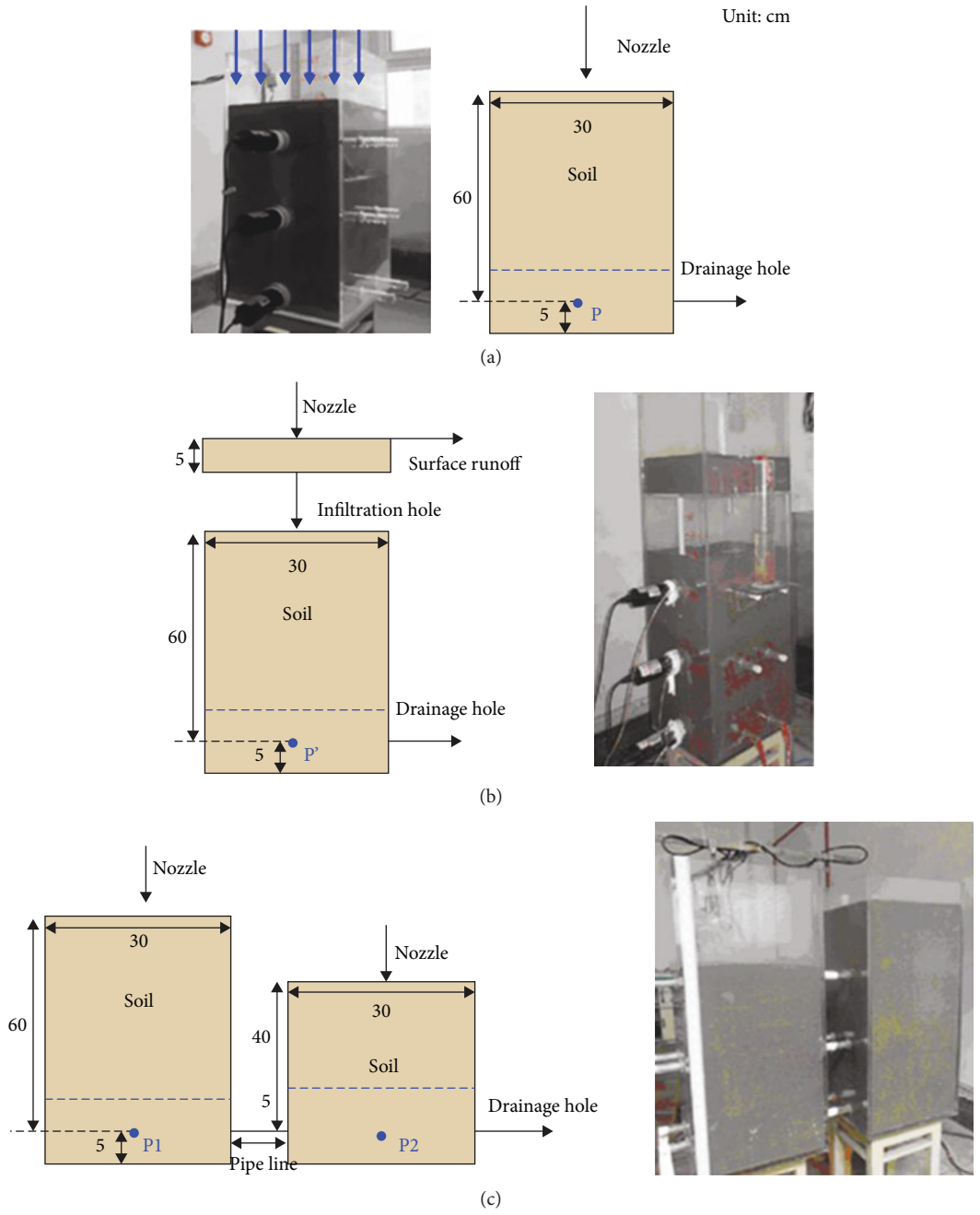

FIGURE 1: Physical tank model experiments (P, P', P1, and P2 are pore water pressure sensors): (a) simple tank model; (b) surface runoff tank model; (c) lateral water flow supply tank model.

In this test, four measuring glasses were randomly placed in the rainfall zone. The applied three rainfall events had rainfall intensities of 25, 45, and 65 mm/hr lasting for 30 min. The uniformity coefficients were calculated as 0.84, 0.88, and 0.90, respectively.

2.1.5. Pore Water Pressure and Drainage Records. To record the pore water pressure, PWP, two pore water pressure transducers (model number CYY2, Xi'an Weizheng Technology Corp. Ltd., Xi'an, China) have been used. Each transducer had a diameter of 3 cm, a height of 1.6 cm, and a measuring range of +10 kPa, with a deviation of 0.2%. A drainage line on the right bottom of the physical tank model was prepared to calculate the drained water. The water was collected using measuring glasses. A video camera recorded the level of water inside the measuring glasses during the test (Figure 5).

Calibration of pore water pressure transducers is necessary before the experiments. A tank ($300 \times 300 \times 700$ mm) was employed for the calibration of the pore water pressure transducers. The transducers were placed in the bottom of the tank. Every time a 3 cm height of the water table was added at the top of the tank, the monitoring value of the transducers was recorded (the output of the transducers is electric current). The graph of applied pore water pressure

Figure 2: Soil being filled into the tank model. Every 5 cm depth soil layer is pressed by the flat.

values against the current values recorded by the PWP transducers is shown in Figure 6.

2.1.6. Data Collection and Software. We used a data acquisition system (Figure 7) (CK01L0R-C20 type) that adopts the RS485 communication interface, which supports long-distance data transmission transferring the recorded data by transducers to a computer. The system uses a MODBUS-RTU protocol and has high data transmission stability, versatility of the multichannel analog input, and 14-bit ADC precision. The collected data is an electric current (0-20 mA) which comes from the transducers.

A software designed by VC++ displayed real-time data and dynamic curves. The interface of the software is divided into three main parts (Figure 8). The left top box represents the real-time value of the water pressure, the top right part produces the monitor data graphs, and in the lower part, the original signals are displayed. The software functions include defining the units, producing the monitor data graph, recording data, and adjusting the monitoring time interval.

2.1.7. Testing Material. The soil material used in the experiments was collected from the toe of Ming Mountain, near the Yangtze River Bank, Chongqing, China (Figure 9). Ming Mountain is located at the Three Gorges Reservoir Area, where the average annual rainfall is 1074.6 mm and 70% of the annual rainfall occurs between May and September. The soil was relatively homogenous and consisted of quaternary alluvial materials.

~500 kg of soil materials was collected for conducting experiments. The materials were sieved through a no. 4 (4.75 mm) size sieve for removing the gallets. The soil's particle-size distribution curve is shown in Figure 10. The soil is classified as silty clay in which 90% of particle-size concentrates are in a range of 0.1-0.4 mm. The initial density of materials was determined as 1.82-1.85 g/cm^3, while the saturated density was calculated as 2.04-2.07 g/cm^3.

2.2. Experiment Procedures. In this study, three types of conceptual tank models for three typical slopes were considered (Figure 1). Every test was conducted under similar initial conditions, such as geometry (cuboid), material (silty clay), moisture content, and initial groundwater level (PWP) (0.6-0.75 kPa, deviation +3%). In each test, the PWP sensor at the bottom of the tank recorded the changes of PWP during the rainfall events. The measuring glass collected the drainage.

2.2.1. Simple Tank Experiment. A total of 7 tests were conducted applying the simple tank model. The experiments included fixed and variable rainfall intensity-duration inputs for the hydrology calculations which are given in Table 2. For example, test 1 simulated a 25 mm/hr (36 min) rainfall event, while test 4 simulated the rainfall events of 25 mm/hr (12 min), 65 mm/hr (12 min), and 25 mm/hr (12 min). The arrangements are aimed at testing the pore pressure under different (variable) rainfall durations and intensities and reconcile the theory with the experimental results.

2.2.2. Surface Runoff Tank Experiment. Surface runoff tank experiments were conducted to investigate how the maximum infiltration rate controls the PWP production in the slope mass by reducing rainfall infiltration. A total of 3 tests were conducted at different rainfall intensities of 25, 45, and 65 mm/hr, and each rain event last for 24 min as shown in Table 3.

2.2.3. Lateral Water Flow Supply Tank Experiment. In addition, two tests were conducted using the lateral water flow supply tank experiment to investigate how lateral flow affects the PWP in both tanks (Table 4). Test 1 simulated a 45 mm/hr (24 min) rainfall event, while test 2 simulated the rainfall event of 65 mm/hr (36 min).

3. Results and Analysis

3.1. Simple Tank Experiment. The pore pressure is proportional to the groundwater level, and the simple tank experiment modal can be written as

$$H_{i+1} - H_i = r_i - d_i, \tag{2}$$

$$d_i = a \cdot H_i, \tag{3}$$

where H_{i+1} and H_i are the groundwater levels at time $i+1$ and i, respectively; r_i and d_i are the rainfall and drainage at time i, respectively; and a is the parameter. Equations (2) and (3) show the process of rainfall-triggered groundwater pressure. For the model construction, understanding the relation between two parameters of rainfall and drainage can predict the changes of pore pressure. It is unnecessary to know the process parameter clearly like water flow velocity and suction. Figure 11 shows the PWP and drainage during tests 1-7 (Table 2). The PWP in the whole processes can be divided into three stages: (1) the initial stage without an

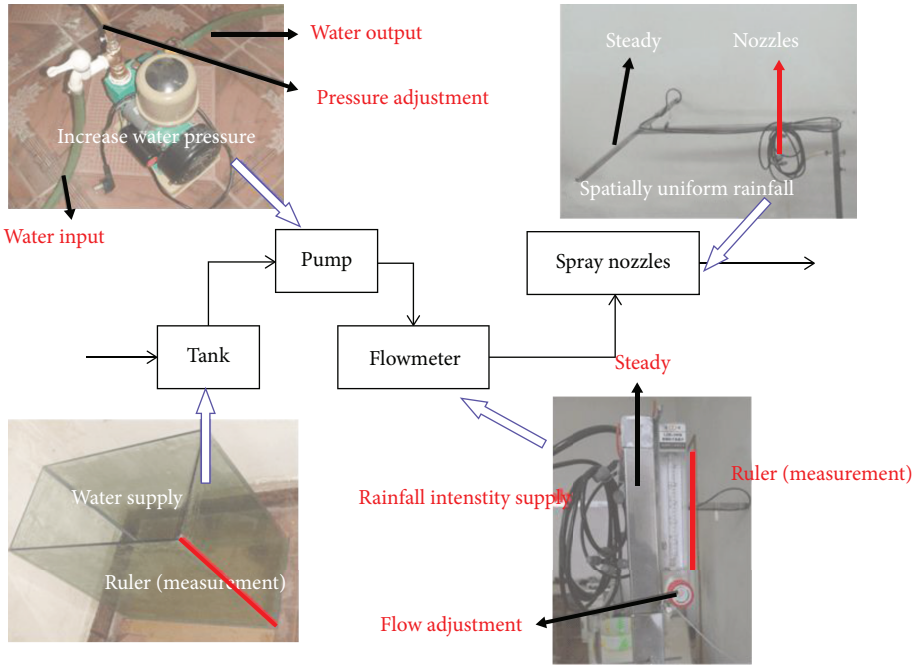

Figure 3: Rainfall simulator systems. They include a water supply (tank with ruler), a water output (pump), a rainfall intensity adjustment (flowmeter), and a rainfall output (spray nozzles).

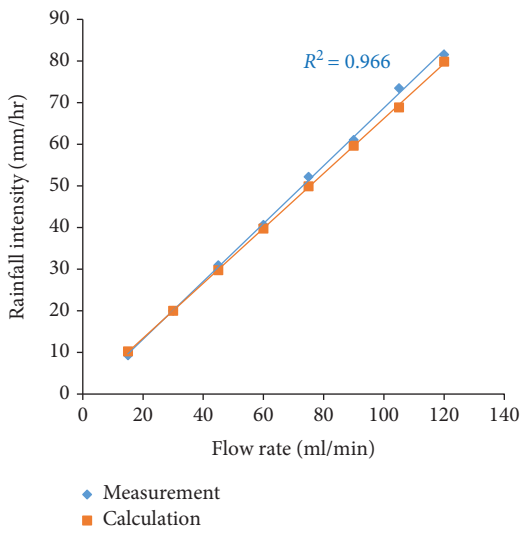

Figure 4: Rainfall intensity simulation test (measured rainfall intensity vs. applied rainfall intensity under different flow rate inputs).

obvious increase in PWP, (2) the second stage with a significant increase in PWP due to the impact of infiltration, and (3) the third stage with a decrease in PWP due to drainage. Figure 11(a) represents the variation of PWP during the experiment for tests 1 to 4. It can be observed that the peak values of PWP varied from 0.7 to 1.6 kPa, while the peak times of PWP varied from 36 to 40 min. Figure 11(b) indicates the variation of PWP during the experiment for tests 5 to 7. In these tests, the peak values of PWP changed from 0.9 to 1.3 kPa while peak times of PWP changed from 30 to 40 min. On the other hand, Figures 11(c) and 11(d) show the variation of drainage. The peak values of drainage rates for tests 1 to 4 were determined from 10 to 50 ml/min at the peak times from 30 to 50 min (Figure 11(c)), while the peak values of drainage rates for tests 5 to 7 were determined from 5 to 30 ml/min (Figure 11(d)) at the peak times from 24 to 40 min. It is found that the amount of rainfall affects the value and time of the PWP peak. Simply, a high rainfall value means a short time lag and a high value of the PWP peak.

Figure 12(a) investigates the relation between PWP and cumulative rainfall of test 3. In the initial stage, the value of PWP due to cumulative rainfall was increased constantly with a very small rate while at the second stage (increase stage), a significant rise in PWP was observed. The PWP decreased at the third stage (decrease stage) where the stage involves the power or exponent function. Degrees of correlations between PWP and cumulative rainfall in the initial, increase, and decrease stages were 0.93, 0.96, and 0.92, respectively. The relationship between drainage rate and PWP in test 3 is given in Figure 12(b). The figure demonstrates a linear relationship between PWP and the drainage rate with the correlation degree of 0.987. It can be observed that a higher PWP caused a faster drainage than a lower PWP.

From equation (2), H_{i+1} and H_i calculated by r_i and d_i are not accurate due to the rainfall time lag in the soil mass, while, in the original conceptual model, the tank model is empty without materials. Thus, equation (2) has no consideration of the time lag. The suggestion is adding a parameter between pore pressures and rainfall drainage to reduce the error. For shallow landslides, the time lag error may not be as obvious as deep-seated landslides. For the drainage, due

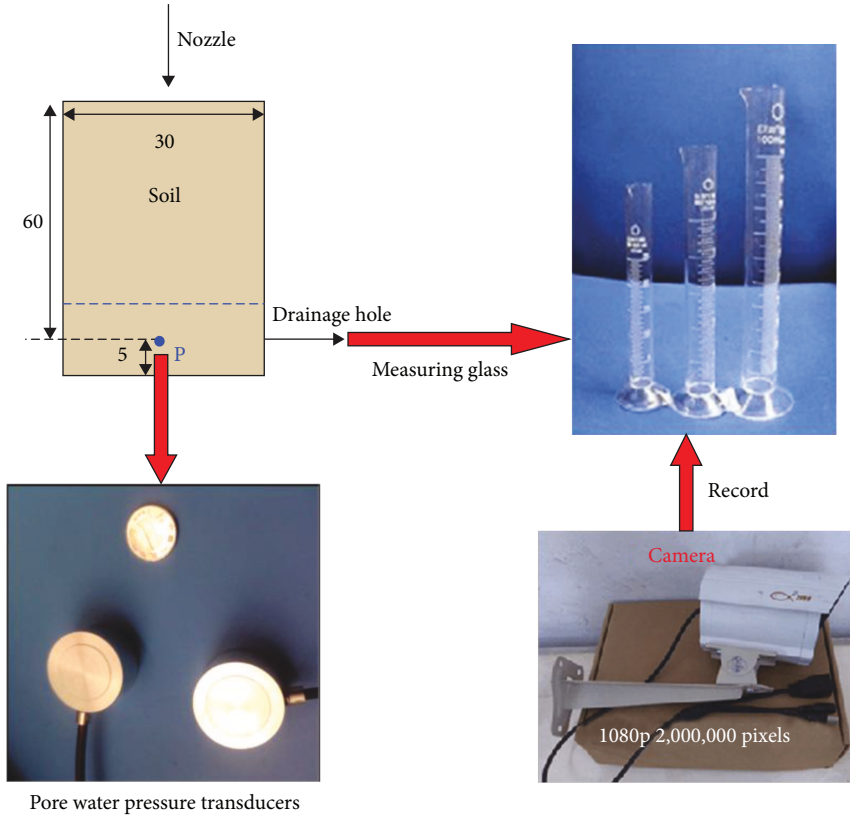

Figure 5: Pore water pressure and drainage records.

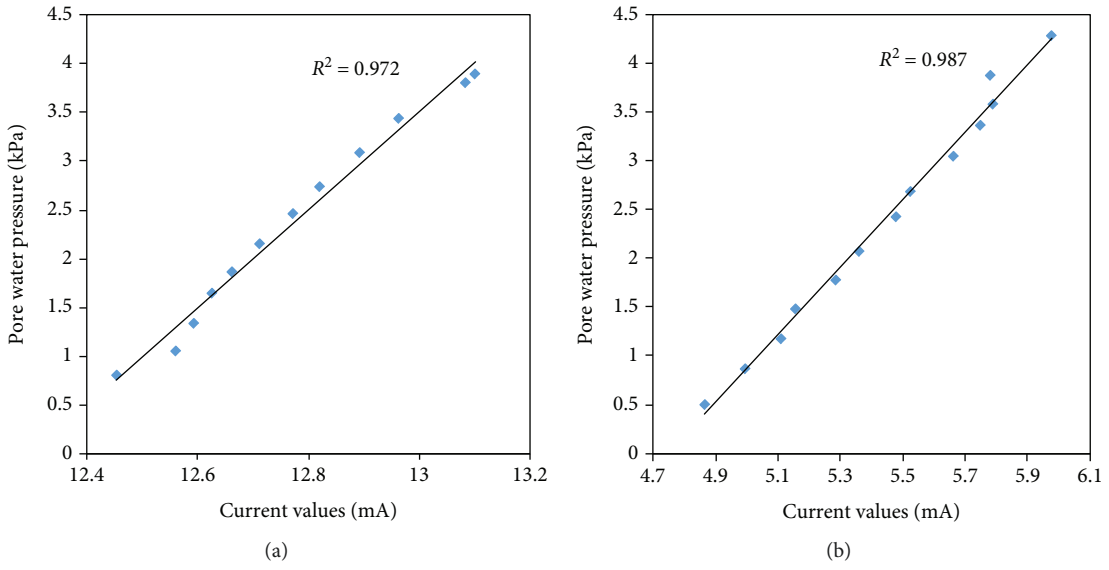

Figure 6: Pore water pressure sensor calibration.

to the less time lag effect of groundwater level reduction in the soil mass, equation (3) can basically describe the process accurately. Thus, the improvement of the model based on the pore pressure parameter can be written as

$$P_{i+1} - P_i = a1 \cdot (r_i - d_i), \quad d_i = a2 \cdot P_i, \tag{4}$$

where P_{i+1} and P_i are the pore pressures at times $i+1$ and i, respectively; r_i and d_i are the rainfall and drainage at time i, respectively; and $a1$ and $a2$ are the parameters.

3.2. Surface Runoff Tank Experiment. For the surface runoff tank experiment, equation (5) would be added to

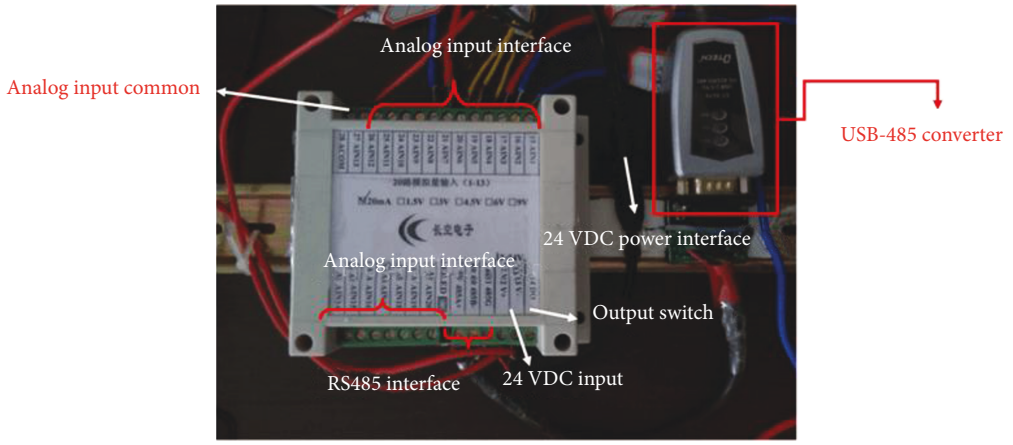

Figure 7: Data acquisition system. It includes an analog input interface, a 24 VDC power interface, and a USB-485converter.

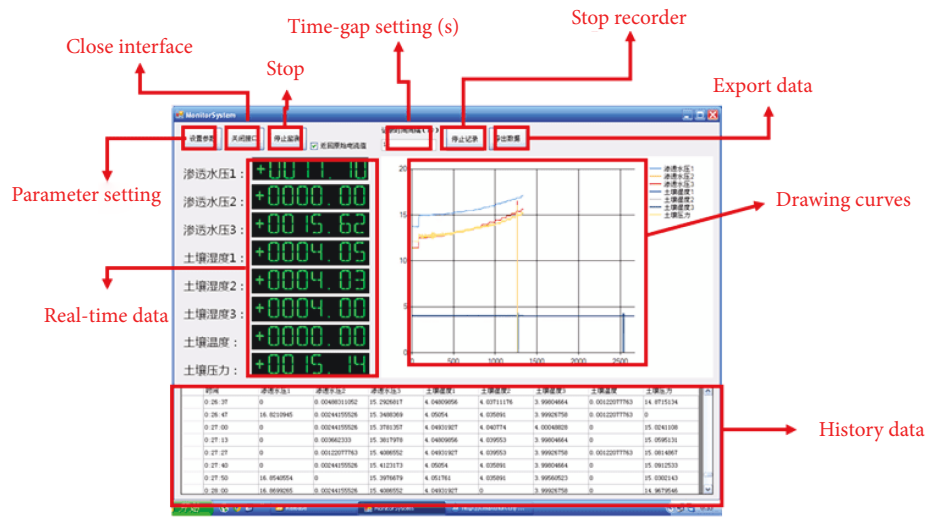

Figure 8: Software for displaying monitoring data.

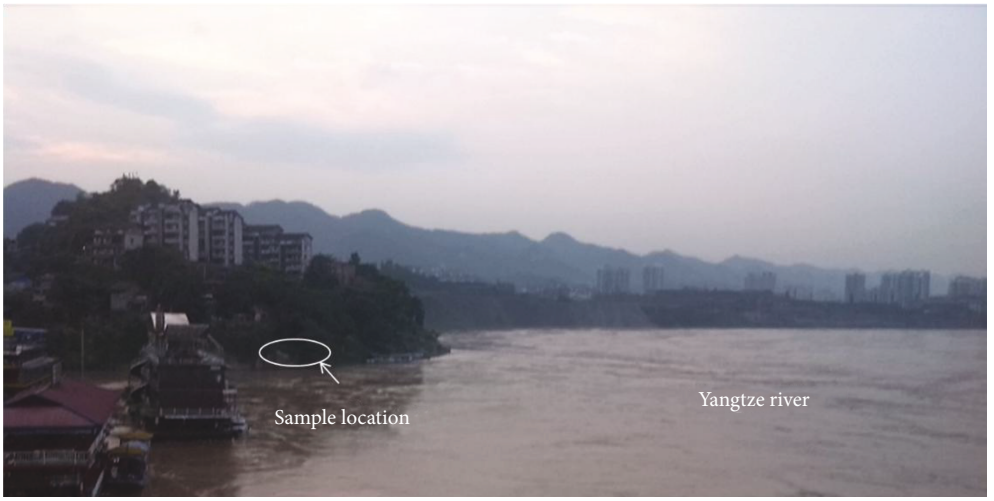

Figure 9: Soil sample location. They were collected from the toe of Ming Mountain, near the Yangtze River Bank, Chongqing, China.

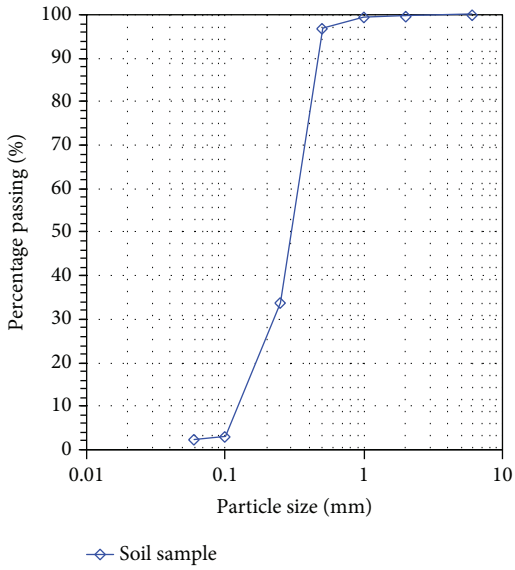

Figure 10: Particle-size distribution curves of the used soil.

describe the maximum infiltration rate limitation (infiltration capacity):

$$H'_{i+1} - H'_i = i_i - d_i, \tag{5}$$

$$i_i = r_i - b \cdot s_i, \tag{6}$$

$$d_i = c \cdot H'_i, \tag{7}$$

where H'_{i+1} and H'_i are the groundwater tables at times $i+1$ and i, respectively; r_i and d_i are the rainfall and drainage at time i, respectively; b and c are the learning parameters; and i_i means the infiltration at time i. s_i is the surface water runoff at time i. For the model construction, compared to the simple tank model, we just need to consider the infiltration capacity which is mainly decided by the soil hydraulic property. It is unnecessary to know the process parameter clearly like water flow velocity and soil hydraulic property like permeability. Thus, the distinct point between the simple and surface runoff tank experiment is the infiltration capacity. The upper tank has a limited infiltration ability realized by a downward infiltration hole. In other words, if there is heavy rainfall, the upper tank could drain some of the excess rain water as surface runoff. Figure 13(a) shows the variation of PWP vs. time for test numbers 1 to 3. It can be observed that peak values of PWP were from 0.85 to 0.95 kPa at the peak times of 45, 75, and 80 min for 65, 45, and 25 mm/hr rainfall events, respectively. As shown in Figure 13(a), the PWP under the 45 mm/hr and 65 mm/hr rainfall events were lower than the PWP under the same rainfall events during simple tank experiments (Figure 11(a)). The surface runoff in Figure 13(b) shows that infiltration thresholds controlled the rainfall surface runoff. During the rainfall periods, the drainage rates were 60, 25, and 7 ml/min for 65, 45, and 25 mm/hr rainfall events, respectively. For the bottom drainage (Figure 13(c)), the results were similar to the simple tank model, except that the maximum

Table 2: Experiment arrangements of the simple tank model.

No.	Rainfall input intensity (duration)	Output objects
1	25 mm/hr (36 min)	P; drainage
2	45 mm/hr (36 min)	P; drainage
3	65 mm/hr (36 min)	P; drainage
4	25 mm/hr (12 min), 65 mm/hr (12 min), 25 mm/hr (12 min)	P; drainage
5	25 mm/hr (24 min)	P; drainage
6	45 mm/hr (24 min)	P; drainage
7	65 mm/hr (24 min)	P; drainage

Table 3: Experiments of surface runoff tank model.

No.	Rainfall input-intensity (duration)	Output objects
1	25 mm/hr (24 min)	P'; drainage; surface runoff
2	45 mm/hr (24 min)	P'; drainage; surface runoff
3	65 mm/hr (24 min)	P'; drainage; surface runoff

Table 4: Experiments of the surface runoff tank model.

No.	Rainfall input intensity (duration)	Output objects
1	45 mm/hr (24 min)	P1; P2; drainage
2	65 mm/hr (24 min)	P1; P2; drainage

infiltration reduced the amount of drainage. Peak values of drainage rates were 2, 5, and 5 ml/min for the 25, 45, and 65 mm/hr rainfall events, respectively, and peak times of drainage rates were 40, 60, and 63 min for 65, 45, and 25 mm/hr rainfall events, respectively. Figure 13(d) shows the rate of infiltration vs. time. Two types of surface runoff are distinguished: Hortonian overland flow occurs when precipitation exceeds the infiltration rate. Saturated overland flow occurs when the soil has reached complete saturation. It takes 3, 5, and 9 min to make the surface soil become saturated for 25, 45, and 65 mm/hr rainfall events, respectively. Then, the saturated overland flow occurs; thus, all the three rainfall infiltrations are limited around 38 ml/min. It can be seen that the maximum infiltration rate was about 38 ml/min for the 25, 45, and 65 mm/hr rainfall events and this indicates that the maximum hydraulic conductivity could be around 38 ml/min at the soil surface (the thin soil layer in the upper tank).

From equation (5), H_{i+1} and H_i calculated by i_i and d_i are still not accurate due to the rainfall time lag in the soil mass. Using i_i not r_i is necessary to reduce the error including the infiltration rate and time lag, while, in the original conceptual model, the tank model is empty without materials. Thus, equation (5) did not include the time

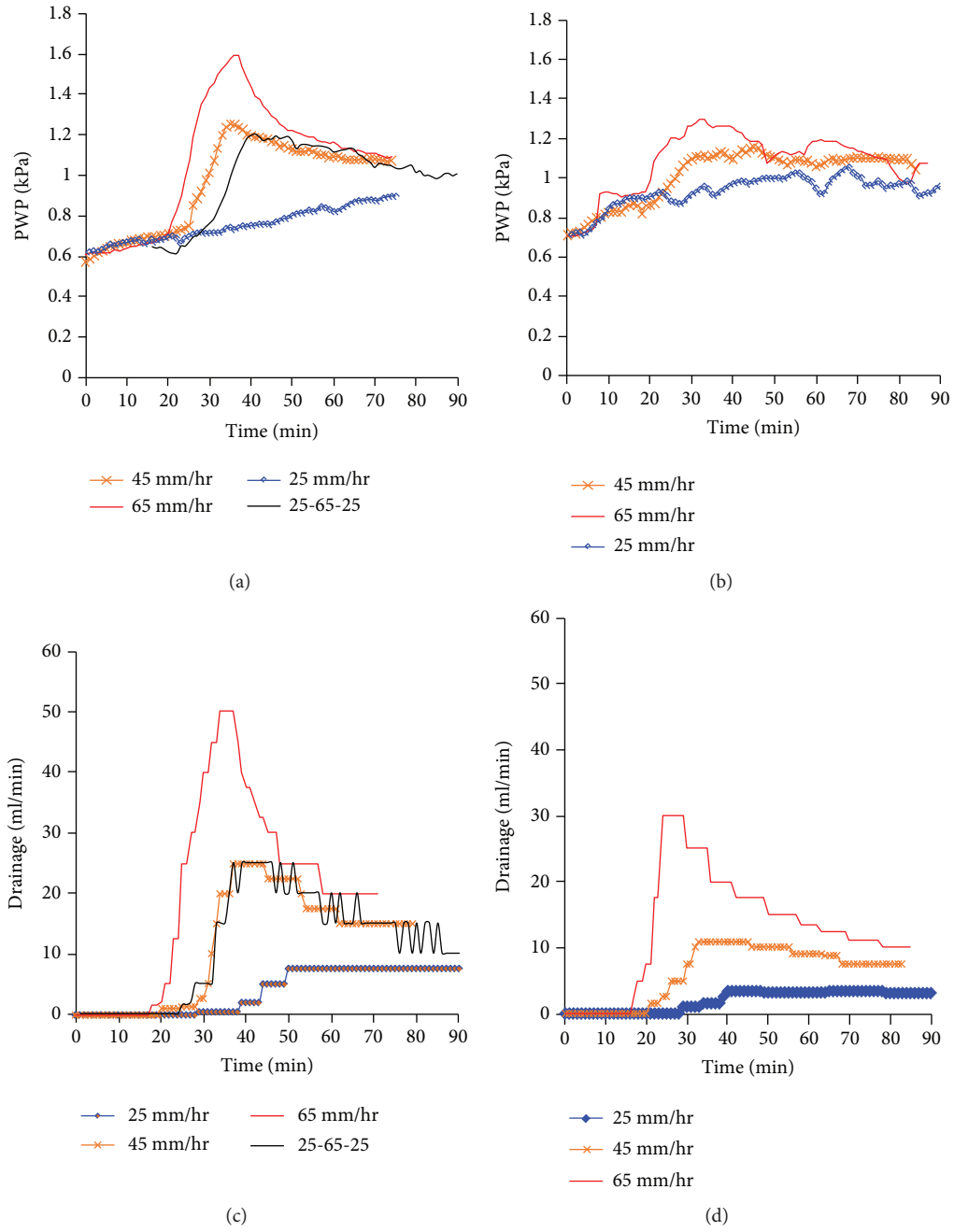

Figure 11: PWP and drainage rate in the simple tank experiments: (a) PWP vs. time for tests 1-4; (b) PWP vs. time for tests 5-7; (c) drainage vs. time for tests 1-4; (d) drainage vs. time for tests 5-7.

lag. The suggestion is adding a parameter between pore pressures and infiltration to reduce the error. A parameter, b, between rainfall and surface runoff is used to adjust the water balance between infiltration and rainfall in equation (6). For the drainage, due to the less time lag effect of the groundwater level reduction in the soil mass, equation (7) can describe the process accurately. Considering the surface runoff, only two parameters a' and b need to be determined by observing the rainfall, drainage, and pore pressure. Thus, it is a straightforward method. The improvement of the model based on the pore pressure parameter can be written as

$$P'_{i+1} - P'_i = b1 \cdot (i_i - d_i), \quad d_i = b2 \cdot P'_i, \tag{8}$$

where P'_{i+1} and P'_i are the pore pressures at times $i+1$ and i, respectively; d_i is the rainfall and drainage at time i; $b1$ and $b2$ are the learning parameters; and i_i means the infiltration at time i.

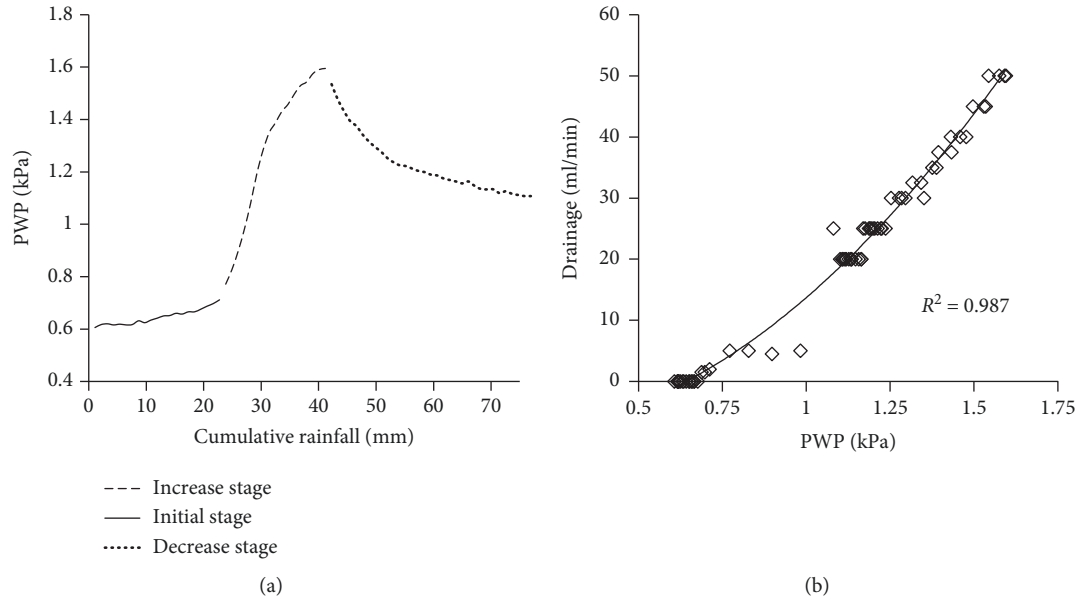

Figure 12: (a) PWP vs. cumulative rainfall (test 3); (b) PWP vs. drainage (test 3).

3.3. Lateral Water Flow Supply Tank Experiment. If the lateral water flow supply is considered, two tank models are necessary for calculation. The conceptual tank model could be

$$H_{1(i+1)} - H_{1i} = r_i - (H_{1i} - H_{2i}), \tag{9}$$

$$H_{2(i+1)} - H_{2i} = r_i - (H_{1i} - H_{2i}), \tag{10}$$

$$d_i = d \cdot H_{2i}, \tag{11}$$

where $H_{1(i+1)}$ and $H_{1i}$are the groundwater tables of the left tank at times $i+1$ and i, respectively; $H_{2(i+1)}$ and H_{2i} are the groundwater tables of the right tank at times $i+1$ and i, respectively; r_i and d_i are the rainfall and drainage at time i, respectively; and d is the learning parameter. For the model construction, compared to the simple tank model, the lateral water flow balance needs to be considered which is mainly dictated by the difference of the pore pressures of both sides. It is unnecessary to know the process parameter clearly like water flow velocity and soil property like permeability. Lateral water flow supply complicates the calculation of the groundwater table especially due to the coupling of the infiltration time lags. Figure 14 illustrates the monitoring data from the PWP sensors and the drainage hole in the lateral water flow supply tank model. From Figure 14(a), it can be observed that the PWP of the right (higher) tank model (P1) increased from -0.1 to 1 and from -0.5 to 2 kPa for the 45 and 65 mm/hr rainfall events, respectively. However, PWP for the right (lower) tank model (P2) was increased from 0.5 to 1.25 and from 0.5 to 2 kPa for the 45 and 65 mm/hr rainfall events, respectively. The maximum values of PWP for both P1 and P2 occurred after 40 to 50 min of the test. The figure shows that the PWP of the right (lower) tank model (P2) firstly begin to increase due to the water supply from the left (higher) tank model. The left tank model as the water supplier mostly affects the right one, although in the beginning, the right one could offer some water to the left one conversely (as shown in Figure 1(c), the right tank's short vertical infiltration path could produce a higher groundwater table than that of the left tank in the beginning). The recorded drainage rates during the test are presented in Figure 14(b). The peak values of the drainage rates are 13 and 45 ml/min for the 45 and 65 mm/hr rainfall events, respectively, which occurred at 35 min after the beginning of the test for both rainfall events.

From equation (9), $H_{1(i+1)}$ and H_{1i} can be calculated by r_i and the lateral water flow supply which is mainly decided by the difference of the pore pressures in both tanks. From equation (10), $H_{2(i+1)}$ and H_{2i} can be calculated by r_i and the lateral water flow supply which is also mainly decided by the difference of the pore pressures in both tanks. As the lateral water flow is under the saturation state, the time lag effect is not obvious, while, in original conceptual model, the tank model is empty without materials. Thus, equations (9) and (10) are suggested to add two parameters ($c1$ and $c2$) between the groundwater pore pressures and lateral water flow pore pressures (Equations (12) and (13)). Considering the surface runoff, only two parameters a and b need to be determined by observing the rainfall, drainage, and pore pressure. Thus, it is a straightforward method. The improvement of the model based on the pore pressure parameter can be written as

$$P_{1(i+1)} - P_{1i} = r_i - c1 \cdot (P_{1i} - P_{2i}), \tag{12}$$

$$P_{2(i+1)} - P_{2i} = r_i - c2 \cdot (P_{1i} - P_{2i}), \tag{13}$$

$$d_i = c3 \cdot P_{2i}, \tag{14}$$

where $P_{1(i+1)}$ and $P_{1i}$are the pore pressures of the left tank at times $i+1$ and i, respectively; $P_{2(i+1)}$ and P_{2i} are

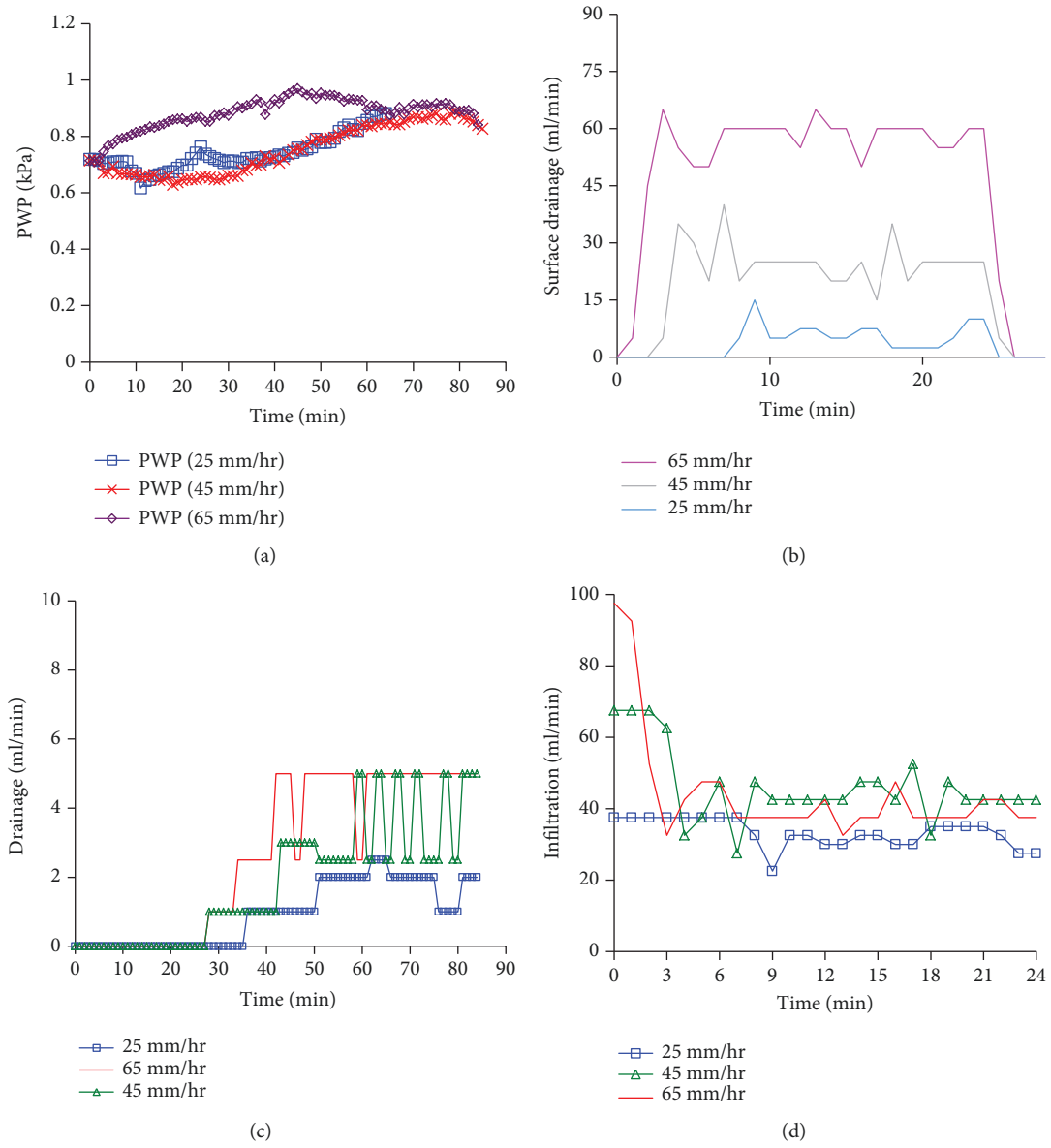

FIGURE 13: Monitoring data from P', surface runoff, and drainage hole (surface runoff tank model): (a) PWP (P') vs. time; (b) surface runoff drainage vs. time; (c) drainage rate vs. time; (d) infiltration rate vs. time.

the pore pressures of the right tank at times $i+1$ and i, respectively; r_i and d_i are the rainfall and drainage at time i, respectively; and $c1$, $c2$, and $c3$ are the parameters.

4. Conclusions

Changes of PWP are controlled by the balancing among the rainfall infiltration, water flow supply, and the drainage. The relationships between PWP on the bottom of the tank, drainage, and rainfall based on three kinds of physical models (the simple tank model, surface runoff tank model, and water flow supply tank model) were investigated. Drainage processes under different rainfall events were also deciphered. Some conclusions are as follows:

(1) The amount of rainfall affects the value and time of PWP peak. Simply, a high rainfall value means a short time lag and a high value of the PWP peak. PWP decreases the effective stress and changes the stress state in the soil that eventually leads to slope failure. In addition, rainfall infiltration replaces the air in the void spaces with water. Since water is heavier than air, this will increase the soil weight. Greater weight means higher stress and being prone to be dragged down by gravity, leading to slope instability. As a result, the increase in the peak PWP will increase the damage to the slope engineering

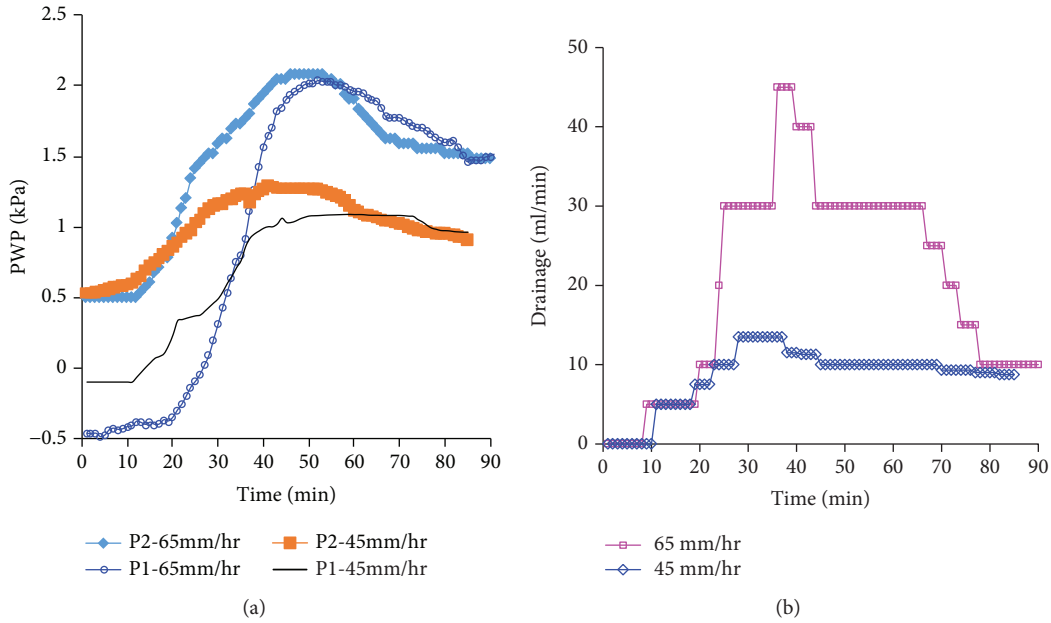

Figure 14: Monitoring data from the PWP sensors and drainage hole (water flow supply tank model): (a) PWP (P1 and P2) vs. time; (b) drainage vs. time.

(2) Infiltration capacity of the surface soil controls the rainfall surface runoff and infiltration capacity. With the decrease of the infiltration threshold, the soil infiltration capacity is reduced and the surface runoff is gradually increased. For the law of rainfall infiltration in the slope mass, understanding the threshold of infiltration of the surface soil is very important

(3) Lateral water flow from a higher part to a lower part of a slope system can fast improve the PWP of the lower part which is mainly dictated by the differences of pore pressure in both sides

(4) The tank model based on the optimized method does not consider the water flow process but needs parameter training. The parameter advance is necessary for setting up the direct links between the pore pressure and rainfall drainage as well as improving the accuracy of the model

Data Availability

Please contact the corresponding author.

Conflicts of Interest

The authors declare that they have no conflicts of interest.

Acknowledgments

The research is partly supported by the National Key R&D Program of China (Grant No. 2017YFC0804601) and the National Natural Science Foundation of China (Nos. 51741410 and 41807286).

References

[1] E. Damiano, R. Greco, A. Guida, L. Olivares, and L. Picarelli, "Investigation on rainwater infiltration into layered shallow covers in pyroclastic soils and its effect on slope stability," *Engineering Geology*, vol. 220, pp. 208–218, 2017.

[2] M. Pirone, R. Papa, M. V. Nicotera, and G. Urciuoli, "Hydraulic behaviour of unsaturated pyroclastic soil observed at different scales," *Procedia Engineering*, vol. 158, pp. 182–187, 2016.

[3] M. Mustafa, M. H. Isa, R. B. Rezaur, and H. Rahardjo, "Data-driven modelling for pore water pressure variation responses to rainfall," in *WIT Transactions on The Built Environment*, vol. 1, pp. 447–455, WIT Press, 2015.

[4] S. K. Kampf and S. J. Burges, "A framework for classifying and comparing distributed hillslope and catchment hydrologic models," *Water Resources Research*, vol. 43, no. 5, 2007.

[5] G. Rianna, L. Pagano, and G. Urciuoli, "Investigation of soil-atmosphere interaction in pyroclastic soils," *Journal of Hydrology*, vol. 510, pp. 480–492, 2014.

[6] W. Shao, T. Bogaard, M. Bakker, and M. Berti, "The influence of preferential flow on pressure propagation and landslide triggering of the Rocca Pitigliana landslide," *Journal of Hydrology*, vol. 543, pp. 360–372, 2016.

[7] N. A. Abebe, F. L. Ogden, and N. R. Pradhan, "Sensitivity and uncertainty analysis of the conceptual HBV rainfall–runoff model: implications for parameter estimation," *Journal of Hydrology*, vol. 389, no. 3-4, pp. 301–310, 2010.

[8] F. Faris and F. Fathani, "A coupled hydrology/slope kinematics model for developing early warning criteria in the Kalitlaga landslide, Banjarnegara, Indonesia," in *Progress of Geo-Disaster Mitigation Technology in Asia*, Environmental Science and Engineering (Environmental Engineering), F. Wang, M. Miyajima, T. Li, W. Shan, and T. Fathani, Eds., pp. 453–467, Springer, Berlin, Heidelberg, 2013.

[9] Y. Ishihara and S. Kobatake, "Runoff model for flood forecasting," *Bulletin of the Disaster Prevention Research Institute*, vol. 29, no. 1, pp. 27–43, 1979.

[10] H. Ohtsu, S. Janrungautai, and K. Takahashi, "A study on the slope risk evaluation due to rainfall using the simplified storage tank model," in *Proceeding of the 2nd Southeast Asia Workshop on Rock Engineering*, pp. 67–72, Bangkok, Thailand, 2003.

[11] K. Takahashi, Y. Ohnish, J. Xiong, and T. Koyama, "Tank model and its application to groundwater table prediction of slope," *Chinese Journal of Rock Mechanics and Engineering*, vol. 27, no. 12, pp. 2501–2508, 2008.

[12] J. Xiong, K. T. Ohnish, and T. Koyama, "Parameter determination of multi-tank model with dynamically dimensioned search," in *Process Symposium Rock Mechanics*, pp. 19–24, Japan, Kyoto, 2009.

[13] W. Bodhinayake, B. C. Si, and K. Noborio, "Determination of hydraulic properties in sloping landscapes from tension and double-ring infiltrometers," *Vadose Zone Journal*, vol. 3, no. 3, pp. 964–970, 2004.

[14] W. Nie, *Estimating and predicting pore-pressure influence on deep-seated landslides, [M.S. thesis]*, Technische Universität München, 2017.

[15] W. Nie, M. Krautblatter, K. Leith, K. Thuro, and J. Festl, "A modified tank model including snowmelt and infiltration time lags for deep-seated landslides in alpine environments (Aggenalm, Germany)," *Natural Hazards and Earth System Sciences*, vol. 17, no. 9, pp. 1595–1610, 2017.

[16] W. Nie, Y. C. Liang, L. Chen, and W. Shao, "Modelling of river-groundwater interactions under rainfall events based on a modified tank model," *Geofluids*, vol. 2017, Article ID 5192473, 11 pages, 2017.